LETTER

The stability of spherocyte membranes: Theoretical study

To cite this article: W. Mu *et al* 2019 *EPL* **128** 38001

A Letters Journal Exploring the Frontiers of Physics

November 2019

EPL, **128** (2019) 38001 www.epljournal.org
doi: 10.1209/0295-5075/128/38001

The stability of spherocyte membranes: Theoretical study

W. Mu[1,2,3(a)], Z-c. Ou-Yang[4] and J. Cao[5,6]

[1] *School of Ophthalmology and Optometry, Eye Hospital, School of Biomedical Engineering, Wenzhou Medical University - Wenzhou 325027, China*
[2] *Wenzhou Institute, University of Chinese Academy of Sciences - Wenzhou 325001, China*
[3] *Department of Electrical Engineering and Computer Science, Massachusetts Institute of Technology Cambridge, MA 02139, USA*
[4] *Institute of Theoretical Physics, the Chinese Academy of Sciences - Beijing 100190, China*
[5] *Department of Chemistry, Massachusetts Institute of Technology - Cambridge, MA 02139, USA*
[6] *Singapore-MIT Alliance for Research and Technology (SMART) - Singapore, 138602*

received 30 July 2019; accepted in final form 13 November 2019
published online 20 January 2020

PACS 87.16.ad – Analytical theories
PACS 87.16.D- – Membranes, bilayers, and vesicles
PACS 87.16.dm – Mechanical properties and rheology

Abstract – Human red blood cell (RBC) membranes are typically biconcave-shaped under physiological conditions, and membranes of other shapes, such as spherical, are also observed in pathological RBCs. It has been suggested that there is a relationship between the RBC membrane's material properties, morphologies and physiological functions. The present work studies how various factors affect the morphologies of the RBC membrane based on a free energy functional in continuum elasticity descriptions. In particular, the instability conditions of a diseased spherocyte's spherical shape is obtained explicitly, which determines the region in the phase diagram constructed by two dimensionless state variables defined by elastic moduli, osmotic pressure, etc., in which the spherocyte's membrane can exist in a stable form. In this phase diagram, each point represents the statistical results for a large number of samples observed in recent experiments. Within this stable region of spherocyte's membrane, the spherical RBC membrane is in the global minimal state whereas in the adjacent region on the other side of the boundary, the echinocyte's membrane corresponds to the global minimal state. Our results could be used as a theoretical guide for clinical applications in related diseases, such as malaria, and are in quantitative agreement with recent dynamic optical measurements on the morphological transition of the RBC membrane (see Park Y. *et al. Proc. Natl. Acad. Sci. U.S.A.*, **107** (2010) 6731).

Red blood cells (RBCs), also called erythrocytes, transport oxygen from the lungs through arteries and capillaries to the tissues and cells. The RBC's physiological function is sensitive to its morphology: a normal healthy RBC has a biconcave shape under physiological conditions, ensuring that it will pass through small blood vessels with reversible deformation, while RBCs with other morphologies lose their physiological functions, leading to serious health disorders, such as malaria [1,2]. Identifying and counting the number of RBCs with the correct morphology can be used in the detection of certain diseases [3]. The normal RBC with a biconcave shape, called a discocyte (DC), is tremendously flexible, while RBCs with other morphologies are not. In particular, the membrane of an RBC that is infected by malaria parasites becomes more spherical. Moreover, the membrane of this abnormal RBC is harder than the normal one, with a typical stiffness 50 times greater than that of a normal biconcave RBC, leading to great difficulty in passing through capillaries by reversible deformation [1,4,5]. As is well known, malaria has been a serious threat to human health since ancient times [4,6] and the disease is still a focus of medical studies. In particular, the 2015 Nobel Prize was bestowed on researchers for finding medicines to treat this disease [7]. Obviously, it is highly desirable to explore the relationships between morphologies and mechanical properties of RBC membranes, in both experimental and theoretical studies [1,8–35]. The shape of an RBC is governed by its

(a) E-mails: muwh@wibe.ac.cn, whmu@mit.edu

mechanical properties, the pressure difference across its membrane, and its size. In the present work, we will study the relationship between the equilibrium shapes and the elastic properties of RBCs in detail. We demonstrate that an experimentally observed shape of an RBC membrane corresponds to a stable equilibrium point in the free energy landscape by the minimum free energy principle in thermodynamic theory, which can be determined by the variational method [36,37]. As an important application of the present theoretical method, we focus on the stability of the abnormal spherocyte, and show the condition for its morphological instability. Various efforts have been made to study the mechanical properties of RBC membranes. At first, static mechanic responses of RBC membranes were investigated extensively by micropipette techniques [16], electric field deformation [12], and optical tweezer techniques [38]. Dynamically, the RBC membrane constantly fluctuates with an amplitude of the order of hundreds of angstroms [13]. The fluctuations depend on the membrane structure and elasticity as well as on the concentration of adenosine triphosphate (ATP) [14,30]; thus, it is possible to extract the properties of the RBC membranes from the dynamical information. The simple intracellular structure of the RBC with its lack of nuclei and other internal structures leads to a uniform refractive index of the entire cell and makes it possible to accurately measure the dynamics changes of the thickness of RBC membrane by noninvasive dynamical optical measurement techniques, and to record the fluctuations of the membrane [24,25]. This paves the way to extracting mechanical characteristics through the dynamic undulations of the RBC membrane [10,19,20,29]. Among the efforts to measure RBC membrane fluctuations, Park *et al.*, in particular, achieved a full-field measurement of membrane fluctuations of RBCs up to the nano-meter scale with morphologies from normal DCs to echinocytes (ECs, spiculate shape) and spherocytes (SCs, nearly spherical shape), as shown in fig. 1, using the optical interferometric technique [24,25]. These results have aroused great interest since they were reported.

The most interesting point of Park *et al.*'s work is that these authors directly obtained the properties of a variety of RBCs in the solution simultaneously, observed the RBC membranes in cell populations, which made it possible to study the morphology-mechanical properties of RBC membrane relationship by investigating the statistical properties of numbers of RBCs in the three main morphologies. The technique avoids the diversity of reported properties of RBC membranes that occurs in experiments focusing on the dynamical morphological evolution of one selected RBC, owning to the cell's individual characters. Their observations revealed that the harder the membrane is, the more likely it is that the RBC is a spherocyte, a pathological form that lacks some physiological functions, such as the ability to carry oxygen. Although this is intuitive, the quantitative theory connecting the mechanical properties of the RBC membrane and the morphology of RBCs, in particular, needs to be established. The physical

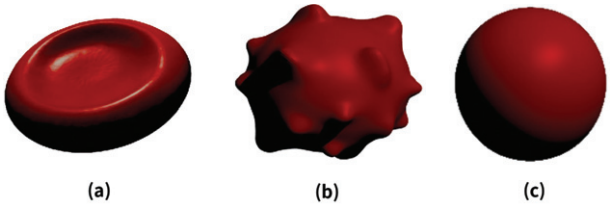

Fig. 1: Schematic sketch of the three morphologies. (a) A normal RBC with a biconcave shape, named a DC; (b) an EC characterized by its stipulate shape; (c) a SC with a nearly spherical shape. The spherocyte is related to particular diseases.

implication of this quantitative relationship is twofold: based on it, we may develop a fast and minimally invasive technique to diagnose certain diseases related to red blood cells; on the other hand, by understanding this relationship, we may develop a treatment method that involves modulating the lipid/cytoskeleton biological structure of the membrane of an infected cell by adjusting the stiffness of the membrane. This may lead to at least partially recovering of the morphological functions of the RBCs. To study the physical mechanisms of equilibrium morphologies and their transitions, first, we briefly introduce the structure of the RBC membrane, since the mechanical properties of the RBC membrane depend on the composite structure of the phospholipid bilayer which is enforced by the cross-linked cytoskeleton [9–11,39,40]. The hexagonal cytoskeleton of the RBC membrane is composed of tetramers of the protein spectrin, which are attached to one another with junction complexes to form a network tethered to the lipid bilayer by the protein ankyrin (see ref. [39] and the references therein). The RBC membrane inherits both fluidity and solid-like mechanical properties from the lipid bilayer and the cytoskeleton, giving the composite structure advantages over a single material. The fluidity property of the lipid bilayer determines the RBC membrane's bending modulus [36,40,41], while the spectrin-dominated 2D network both serves as the scaffold maintaining the RBC's shape and mechanical integrity, and dominantly contributes to the elastic modulus of the membrane [19]. Thus, it is necessary to adopt an elastic energy description considering the contribution of both the lipid bilayer and the cytoskeleton [27]. In the present analytical work on the condition for weakening the abnormal spherocyte, we use a continuum elastic body description, and illustrate the basic physics with a model as simple as possible. The elastic energy of the lipid bilayer can be described by the well-established Helfrich energy [41]. This is a functional of the curvatures defined on a 2D curved surface, based on the theory of surfaces in classical differential geometry [42]:

$$E_b = \frac{\kappa}{2} \iint \mathrm{d}^2 s (2H + c_0)^2 + \bar{k} \iint \mathrm{d}^2 s K, \qquad (1)$$

where H and K denote the mean and Gaussian curvatures of the surface reprenting the membrane, and κ ($\bar{k}$) denotes

Table 1: Properties of RBC membrane at various morphological phases, experimental data taken from ref. [25].

	DCs	DCs(-ATP)[a]	ECs	SCs
$\kappa(k_{\rm B}T)$	5.5 ± 1.7	6.7 ± 3.3	9.6 ± 3.2	23.9 ± 6.7
$\mu(\mu{\rm Nm}^{-1})$	7.4 ± 0.9	≈ 9	10.4 ± 2.9	12.6 ± 2.1
$K_A(\,\mu{\rm Nm}^{-1})$[b]	15.5 ± 2.5	23.9 ± 8.3	31.7 ± 10.0	41.8 ± 10.3
$S(\,\mu{\rm m}^2)$[c]	139.4	–	143.4	96.3
$\sqrt{\langle \Delta h^2 \rangle}(\,{\rm nm})$[d]	46	–	34	15

[a] ATP depleted DCs.
[b] Area modulus, $K_A \equiv \lambda + \mu$.
[c] Surface area.
[d] Mean squared normal displacement.

the corresponding mean (Gaussian) curvature modulus. For a closed surface, the latter integral in eq. (1) merely provides a constant, $2\pi\bar{k}\tilde{\chi}$, where $\tilde{\chi}$ is the Euler characteristic, according to the Gauss-Bonet theorem [42], implying that only the term of mean curvature (with a typical modulus, $\kappa \sim 1 - 10\,{\rm k_B T}$) in eq. (1) is nontrivial among the elastic energy expressions of the RBC membrane. The Helfrich energy differs from the previous curvature energy description by including the spontaneous curvature, c_0, which was introduced to describe the effects of the different solution environments inside and outside the membrane [41]. The spectrin-based cytoskeleton in the RBC membrane is a homogeneous 2D lattice coupled to a lipid bilayer, which can be modeled as a 2D elastic continuum with the in-plane strains $\varepsilon_{i,j}$, $(i, j = 1, 2)$ [43],

$$E_e = \iint {\rm d}^2 s \left\{ \frac{K_A}{2}(\varepsilon_{11}+\varepsilon_{22})^2 + \mu \left[\frac{(\varepsilon_{11}-\varepsilon_{22})^2}{2} + 2\varepsilon_{12}^2 \right] \right\}. \quad (2)$$

Here, the "inverse of K_A" and μ the area compressibility and shear modulus, respectively [15,44]. Elastic models with more biological details of RBCs were proposed in refs. [17,18,22,26,33,35] and the references therein, in order to describe both the static phenomena and dynamic responses of RBC membranes. We use the present simple model, instead, since most of the parameters in our model are observables measured in the related dynamic optical experiments, and there is no adjustable parameter. For simplicity, the mean values of the observed moduli are used. In ref. [25], the elastic properties of a number of RBC membranes with certain morphologies, *i.e.*, both normal and abnormal cells, are reported. The main information is summarized in table 1, which gives the mean values of the experimental data (cf. fig. 4 in ref. [25]). The values presented in table 1 come from the statistics of the reported experimental data, in order to avoid the uncertainty of the moduli caused by individual differences of RBCs.

The total free energy includes Helfrich elasticity, the in-plane elastic energy and the surface tension energy, as well as the pressure difference term, taking the form of

$$F = E_b + E_e + \gamma S + \Delta p V. \quad (3)$$

Here, the surface tension coefficient of the RBC membrane, γ, is assumed to be a constant at room temperature [36], and $\Delta p \equiv p_{\rm out} - p_{\rm in}$ is defined as the pressure difference across the RBC membrane. This free energy functional is based on a model with a minimum set of parameters which gives a clear physical picture of the formation of the main equilibrium shapes of RBC membranes and quantitatively explains the observed morphological transitions of SCs-ECs-DCs [25]; thus it is suitable for the present study. An equilibrium shape of an RBC membrane corresponds to a minimum of the free energy described by eq. (3), determined by the variational equation $\delta^{(1)}F = 0$. The variation $\delta^{(1)}F$ is a function of the mean curvatures of the curved surface, H, whereas the mean curvature itself is a function of the coordinates. Thus the shape equation $\delta^{(1)}F = 0$ is a highly nonlinear differential equation, usually difficult to solve analytically, except for some special solutions with certain symmetries. Among these highly symmetric cases, the spherical membrane of a spherocyte gives the simplest solution of the shape equation (for more information on the details of mathematical deriving see Supplementary Material `Supplementarymaterial.pdf` (SM))

$$\Delta p R^2 + (4K_A\varepsilon + 2\gamma)R + \kappa c_0(c_0 R - 2) = 0, \quad (4)$$

where R is the radius. The existence of this spherical surface solution was confirmed by experimental observations. Here, we assume isotopic 2D in-plane strains in the spherical RBC membrane, $\varepsilon_{11} = \varepsilon_{22} = \varepsilon$, $\varepsilon_{12} = 0$, for the consistency of the spherical symmetry of the free energy, variational equation (shape equation) and the special solution. We then focus on the conditions for weakening the pathological spherocyte's membrane, since this is closely related to the recovery of its physiological functions. Thus, this investigation into the stability of the spherocyte's membrane has implications for both biomedical research and applications. The stability is studied

$$\delta^{(2)}F = \sum_{lm}\left\{\frac{(l+2)\,(l-1)\left[\kappa l(l+1)-\kappa c_0 R-\Delta p R^3/2\right]}{R^2}+4K_A\right\}|a_{lm}|^2\,,\qquad l=0,1,\ldots,\infty,\quad m=-l,\ldots,l. \tag{5}$$

using perturbation analysis for the radial distortion, up to $O(\psi^2)$. This distortion along the normal direction of a spherical surface depends on the polar and azimuthal angle in the spherical coordinates, θ and ϕ, which can be expanded on the basis of the spherical harmonics, $\{Y_{lm},\, l=0,1,\ldots,\infty,\, m=-l,\ldots,l\}$,

$$\psi(\theta,\phi)=\sum_{l=0}^{\infty}\sum_{m=-l}^{l}a_{lm}Y_{lm}(\theta,\phi),$$

with the magnitude $a_{l,-m}=a_{lm}^*$ to ensure that the coefficients $\{a_{lm}\}$ are real. Here the asterisk in superscript indicates the complex conjugation operation. A spherocyte's memebrane at thermodynamic equilibrium satisfies the shape equation in eq. (4). This implies that, at equilibrium, the isotropic strain ε is not independent; thus, in the second order of the variation of the total free energy, the isotropic stain can be eliminated, leading to (see SM)

see eq. (5) *on top of the page*

A spherocyte's membrane can maintain its spherical symmetry under the normal distortion $\psi(\theta,\phi)$, if $\delta^{(2)}F>0$, $l\geq 2$; otherwise, it may deform to a shape with a lower symmetry, resulting in instability. The critical condition for the morphological transition $\delta^{(2)}F=0$, $l\geq 2$ gives a series of possible critical pressure differences across the membrane,

$$\Delta p_1=\frac{2\kappa l(l+1)}{R^3}+\frac{8K_A}{R[l(l+1)-2]}-\frac{2\kappa c_0}{R^2},\qquad l=0,1,\ldots. \tag{6}$$

Then, it is convenient to introduce a dimensionless quantity $\eta\equiv K_A R^2/\kappa$, define a new integer variable $y\equiv l(l+1)-2$, and rewrite eq. (6) as

$$\Delta p_1=\frac{2\kappa}{R^3}\left[y+\frac{4\eta}{y}\right]+\frac{4\kappa}{R^3}-\frac{2\kappa c_0}{R^2}\geq\frac{8\kappa\sqrt{\eta}}{R^3}+\frac{2\kappa}{R^3}(2-c_0R). \tag{7}$$

The inequality in eq. (7) originates from the arithmetic geometric average inequality $a+b\geq 2\sqrt{ab}$, for any two positive numbers a and b. The inequality is valid since the $(2-c_0R)>0$ for the $c_0R\approx -1.618$, much close to the opposite of golden ratio $\phi=(1+\sqrt{5})/2\approx 1.618$ [37]. Although spontaneous curvature c_0 describes the effect of difference environments inside and outside of the membrane, thus is important to determine the equilibrium shape of a RBC's membrane, the fact that c_0R is nearly a constant leads to c_0 is not a sensitive parameter of our present stability analysis.

A spherocyte's membrane with a certain bending modulus, spontaneous curvature, and radius is thermodynamically stable if the osmotic pressure $\Delta p\leq\Delta p_1(y)$. The y dependence of the reduced pressure (a dimensionless variable) $\bar{p}_1\equiv\Delta p_1/(2\kappa/R^3)$ for three typical sets of parameter shown in fig. 2 demonstrates a minimum $\bar{p}_{1,\,\min}$ in each curve. The stability condition of Δp for a spherocyte's membrane is satisfied for all $l\geq 2$ if $\Delta p_1\leq(2\kappa/R^3)\bar{p}_{1,\,\min}$. As shown in fig. 2, the reduced pressure $\bar{p}_1$, and hence Δp_1, can reach its minimum $\Delta p_{1,\,\min}$ as shown by the inequality of eq. (7) under the experimental conditions [25]. By defining a dimensionless quantity $\xi\equiv\Delta pR^3/\kappa$, the condition for the existence of a stable spherocyte's membrane can be described as

$$\xi(p_{1,\,\min})=\sqrt{\eta}+2(2-c_0R). \tag{8}$$

Instability of a spherocyte's membrane may occur when the osmotic pressure $\Delta p_1>\Delta p_{1,\,\min}$. Under physiological conditions, the value of the osmotic pressure is $\Delta p_0\approx 1.5\,\mathrm{Pa}$ [21]. This implies that if $\Delta p_{1,\min}<1.5\,\mathrm{Pa}$, the spherocyte's membrane can no longer maintain its spherical symmetric shape ($l=0$), and high-order spherical harmonic modes occur, leading to a morphological transition to a new preferable shape. As shown in fig. 2, the value of y for the $\bar{p}_{1,\,\min}$ is $\sim 10^2$, corresponding to $l\approx 10$, under the experimental conditions. If a spherocyte's membrane becomes thermodynamically unstable,

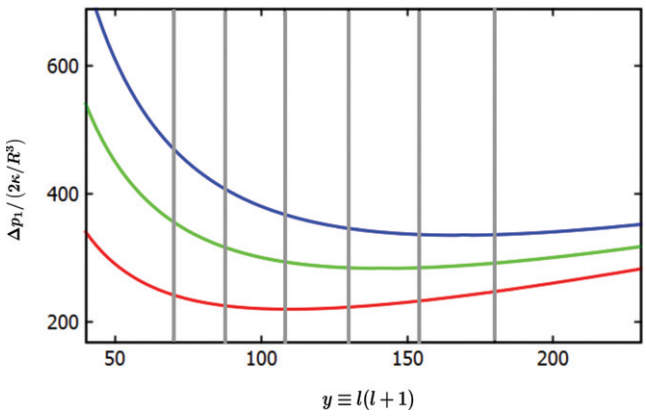

Fig. 2: Relationship between the reduced pressure (a dimensionless quantity) $\bar{p}_1\equiv\Delta p_1/\left(2\kappa/R^3\right)$ and the integer $y\equiv l(l+1)-2$. Here $(c_0R=-1.618)$ [37], and we use the approximate relationship $c_0R=-1$ for simplicity. The three curves are for the typical values of the dimensionless quantity $\eta\equiv K_AR^2/\kappa$, ranging from 3000 to 8000 [25], with $\eta=3000$ for the red line, $\eta=5000$ for the green line, and $\eta=7000$ for the blue line. The integer $y\equiv l(l+1)-2$ values from 70 to 180 ($l=8$–13) are labelled with a series of perpendicular gray lines, and the minima for the three curves all fall within the present range 70–80 of integers $y\equiv l(l+1)-2$.

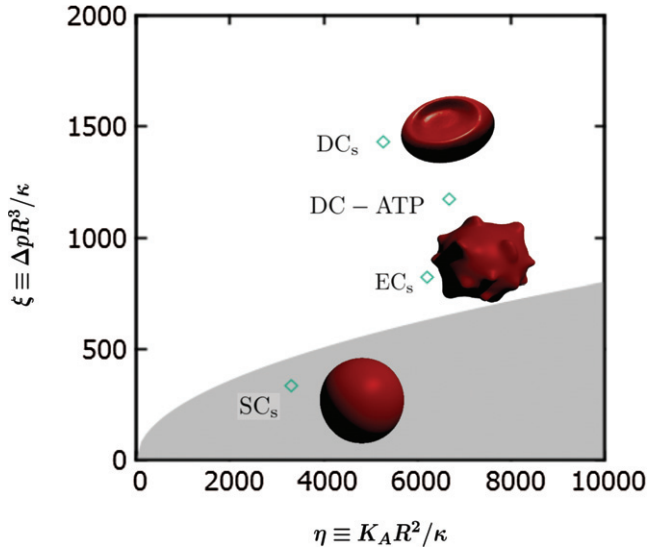

Fig. 3: Phase diagram of RBCs of several manifest morphological types. The boundary curve of the shadow area is described by the stability condition for a spherocyte's membrane shown in eq. (8). The dots denote the corresponding values of the physiological osmotic pressure $\Delta p_0 = 1.5\,\mathrm{Pa}$. In the shadow area, SCs can stably exist. Instability may occur in the area above the boundary curve of the shadow area, thus triggering the morphological transition of SC to EC.

the spherical harmonics with $l = 10$ first occurs, implies the global minimum of free energy functional is shifted to a new one with lower symmetry than that of a spherocyte's. The new global minimum has a $l \gg 1$ spherical harmonic mode, matching the characterized spiculate shape of an echinocyte's memberane, suggesting that a spherocyte's membrane tends to deform to an EC's membrane. This is in agreement with the experiments [25]. Inspired by the stability condition of a spherocyte's membrane obtained in eq. (8), we constructed a phase diagram using two dimensionless quantities, $\xi \equiv \Delta p R^3/\kappa$ and $\eta \equiv K_A R^2/\kappa$. In this 2D phase diagram, all the observed RBC membranes with their elastic and geometric properties can be shown in one figure for easy comparison by taking advantage of the two dimensionless variables composed of K_A, κ, R, and Δp. The phase diagram in fig. 3 clearly shows the region of the stable-existing spherocyte, and suggests possible ways to weaken the stability of the spherocyte and thus promote a transition SC-EC-DC. These include adjusting the osmotic pressure and changing the compressibility of the RBC membrane by modulating the expression of special proteins in the membrane.

So far, we have derived the stability conditions for the pathological spherocyte's membrane shown in eqs. (7) and (8), through a perturbation analysis based on the free energy functional in eq. (3). We demonstrate that the observed equilibrium shape of an RBC's membrane depends on a set of parameters, which corresponds to a global minimum of the free energy landscape under experimental conditions. In general, numerically determining the global minimum of a free energy functional is very difficult; however, since our present study is based on experimental results, we can note that an observed shape of an RBC's membrane does correspond to a solution of the variation equation, $\delta^{(1)}F = 0$ with $\delta^{(2)}F > 0$, which describes a global minimum of the free energy under corresponding experimental conditions. In the present work, we have exploited these experimental data, and expressed RBC membranes with three different morphologies in a 2D phase diagram constructed by two dimensionless variables $\xi \equiv \Delta p R^3/\kappa$ and $\eta \equiv K_A R^2/\kappa$. In the phase diagram shown in fig. 3, each point represents a typical RBC membrane with a certian morphology, based on the mean values of the properties of a number of RBC membrane given in ref. [25]. We have investigated the stability of the pathological spherocyte's membrane through a perturbation analysis, and propose a boundary between the regions corresponding to SC and EC membranes. Our results are in reasonable agreement with the experimental results in ref. [25], which verifies our approach. It is worth mentioning that the morphology of the RBC also depends on the concentration of ATP [25]. The depletion of ATP may affect the coupling of spectrin to the lipid bilayer, resulting in stiffness of the RBC membrane's shear modulus, as in the statistical data based on experiments in ref. [25] shown in table 1. The stiffness of RBC membranes due to ATP depletion was also reported elsewhere in the literature [23,34]. This stiffness of RBC membrane's shear modulus, shifts the values of two dimensionless parameters ξ and η, therefore affects the stability of a spherocyte's membrane. In fig. 3, we show a representative point for the ATP-depleted DC's membrane based on the mean values of measured data for a number of RBCs, which is denoted as DC(-ATP). The present results could be further developed by introducing the ATP concentration-dependent elastic modulus of the RBC membrane into the elastic energy in eq. (2), to quantitatively investigate the influence of cellular ATP on the morphological transition of an RBC membrane. Another interesting topic involving the mechanics of RBC is the interplay of morphological transitions of RBC and the fluidity properties of blood flow. For example, the viscosity of blood increases with increased stiffness of RBCs due to infection, such as occurs in malaria, which places strain on the heart to maintain the blood flow. The shear fluid may in turn alter the morphology of the RBC membrane. Work on viscosity-induced morphological transitions is in progress, using similar approaches to that described in the present work.

In summary, we have studied the morphological transition of a pathological spherocyte through stability analysis of the spherocyte's membrane based on the measurements given in ref. [25] from studies of the relationships between the morphology and the elastic properties of RBC membranes. The present work was inspired by clinical observations in diseases related to RBC morphology and elasticity; for example, a prevalence of spherocytes in

the blood stream, together with stiffening of the RBC membranes, is usually associated with malaria in humans. We suggest a phase diagram for the morphologies of RBC membrane with two dimensionless state parameters, $K_A R^2/\kappa$ and $\Delta p R^3/\kappa$, showing the possible parameter space for the stably existing spherocyte. In general, RBC membranes should be described in a high-dimensional state parameter space, with a series of parameters associated with each membrane, including K_A, κ, and R. However, with the two dimensionless parameters, the state parameter space is reduced to a two-dimensional one, thereby simplifing the stability analysis in order to study the conditions for weakening the stability of a pathological human spherocyte. We also explain the observed transition from SCs to ECs following the development of instability of the spherocyte's membrane. The results are in good agreement with recent experimental measurements of the morphologies and mechanical properties of RBCs [24,25]. Our results could be used as a theoretical guide for the clinical treatment of diseases related to RBC membrane morphology and elasticity, such as human malaria. The present approach could also be used to study more complicated phenomena related to the mechanical properties of RBC membranes and other soft materials, such as viral capsids [45–48].

* * *

WM thanks the National Science Foundation of China (NSFC) (Grant Nos. 11374310), and startup funding of Wenzhou Institute, University of Chinese Academy of Sciences (Grant No. WIBEZD2018001-04). JC acknowledges the financial assistance of Singapore-MIT Alliance for Research and Technology (SMART), National Science Foundation (NSF CHE-112825).

REFERENCES

[1] Fedosov D. A., Caswella B., Suresh S. and Karniadakis G. E., *Proc. Natl. Acad. Sci. U.S.A.*, **108** (2011) 35.
[2] Pivkin I. V., Peng Z., Karniadakis G. E., Buffet P. A., Dao M. and Suresh S., *Proc. Natl. Acad. Sci. U.S.A.*, **113** (2016) 7804.
[3] Ventura B. D., Schiavo L., Altucci C., Esposito R. and Velotta R., *Biomed. Opt. Express*, **2** (2011) 3223.
[4] Mohandas N. and An X., *Med. Microbiol. Immunol.*, **201** (2012) 593.
[5] Zhang *et al.*, *Proc. Natl. Acad. Sci. U.S.A.*, **112** (2015) 6068.
[6] Cunha B. A., *Infect. Dis. Clin. North Am.*, **18** (2004) 53.
[7] Tu Y., *Artemisinin: A Gift from Traditional Chinese Medicine to the World*, `https://www.nobelprize.org/uploads/2018/06/tu-lecture.pdf`.
[8] Fung Y. B. and Tong P., *Biophys. J.*, **8** (1968) 175.
[9] Evans E. A., *Biophys. J.*, **13** (1973) 941.
[10] Brochard F. and Lennon J. F., *J. Phys. (Paris)*, **36** (1975) 1035.
[11] Evans E. A., *Biophys. J.*, **16** (1976) 597.
[12] Engelhardt H., Gaub H. and Sackmann E., *Nature (London)*, **307** (1984) 378.
[13] Zeman K., Engelhardt H. and Sackman E., *Eur. Biophys. J.*, **18** (1990) 203.
[14] Levin S. and Korenstein R., *Biophys. J.*, **60** (1991) 733.
[15] Boal D. H., Seifert U. and Zilker A., *Phys. Rev. Lett.*, **69** (1992) 3405.
[16] Discher D. E., Mohandas N. and Evans E. A., *Science*, **266** (1994) 1032.
[17] Lim H. W. G., Wortis M. and Mukhopadhyay R., *Proc. Natl. Acad. Sci. U.S.A.*, **99** (2002) 16766.
[18] Mukhopadhyay R., Lim H. W. G. and Wortis M., *Biophys. J.*, **82** (2002) 1756.
[19] Fournier J. B., Lacoste D. and Raphael E., *Phys. Rev. Lett.*, **92** (2004) 018102.
[20] Popescu G. *et al.*, *Phys. Rev. Lett.*, **97** (2006) 218101.
[21] Rochal S. B. and Lorman V. L., *Phys. Rev. Lett.*, **96** (2006) 248102.
[22] Auth T., Safran S. A. and Gov N. S., *Phys. Rev. E*, **76** (2007) 051910.
[23] Betz T., Lenz M., Joanny J.-F. and Sykes C., *Proc. Natl. Acad. Sci. U.S.A.*, **106** (2009) 15320.
[24] Park Y. *et al.*, *Proc. Natl. Acad. Sci. U.S.A.*, **107** (2010) 1289.
[25] Park Y. *et al.*, *Proc. Natl. Acad. Sci. U.S.A.*, **107** (2010) 6731.
[26] Park Y. *et al.*, *Phys. Rev. E*, **83** (2011) 051925.
[27] Nans A., Mohandas N. and Stokes D. L., *Biophys. J.*, **101** (2011) 2341.
[28] Efremov A. and Cao J., *Biophys. J.*, **101** (2011) 1032.
[29] Ben-Isaac E., Park Y. K., Popescu G., Brown F. L. H., Gov N. S. and Shokef Y., *Phys. Rev. Lett.*, **106** (2011) 238103.
[30] Loubet B., Seifert U. and Lomholt M. A., *Phys. Rev. E*, **85** (2012) 031913.
[31] Boss D., Hoffmann A., Rappaz B., Depeursinge C., Magistretti P. J., de Ville D. V. and Marquet P., *PLoS ONE*, **7** (2012) e40667.
[32] Xu X., Efremov A. K., Li M. D. A., Lim C. T. and Cao J., *PLoS ONE*, **8** (2013) e64763.
[33] Fedosov D. A., Peltomáki M. and Gompper G., *Soft Matter*, **10** (2014) 4258.
[34] Rodríguez-García I., López-Montero R., Mell M., Egea G., Gov N. S. and Monroy F., *Biophys. J.*, **108** (2015) 2794.
[35] Evans A. A., Bhaduri B., Popescu G. and Levine A. J., *Proc. Natl. Acad. Sci. U.S.A.*, **114** (2017) 2865.
[36] Ou-Yang Z-c. and Helfrich W., *Phys. Rev. A*, **39** (1989) 5280.
[37] Ou-Yang Z-c., Liu J.-X. and Xie Y.-Z., *Geometric Methods in the Elastic Theory of Membranes in Liquid Crystal Phases, Advanced Series on Theoretical Physical Science*, Vol. **2**, 1st edition (World Scientific Publishing Company, Singapore) 1999.
[38] Bao G. and Suresh S., *Nat. Mater.*, **2** (2003) 715.
[39] Boal D., *Mechanics of the Cell*, 2nd edition (Cambridge University Press, New York) 2012.
[40] Evans E. A. and Skalak R., *Mechanics and Thermodynamics of Biomembranes* (CRC Press, Fla., USA) 1980.

[41] Helfrich W., *Z. Naturforsch.*, **28c** (1973) 693.
[42] Kühnel W., *Differential Geometry: Curves-Surfaces-Manifolds*, 2nd edition (American Mathematical Society, USA) 2005.
[43] Zhang Z., Davis H. T. and Kroll D. M., *Phys. Rev. E*, **48** (1993) R651.
[44] Landau L. D. and Lifshitz E. M., *Theory of Elasticity*, 3rd revised edition (Pergamon Press, Oxford, England) 1986.
[45] Quilliet C., Zoldesi C., Riera C., van Blaaderen A. and Imhof A., *Eur. Phys. J. E*, **27** (2008) 13.
[46] May E. R., Aggarwal A., Klug W. S. and Brooks C. L., *Biophys. J.*, **100** (2011) L59.
[47] Quemeneur F., Quilliet C., Faivre M., Viallat A. and Pépin-Donat B., *Phys. Rev. Lett.*, **108** (2012) 108303.
[48] Yong E. H., Nelson D. R. and Mahadevan L., *Phys. Rev. Lett.*, **111** (2013) 177801.